Dalton Transactions

ROYAL SOCIETY OF CHEMISTRY

PAPER

View Article Online
View Journal | View Issue

Cite this: *Dalton Trans.*, 2024, **53**, 4048

New insight into the catalytic mechanism of ester hydrogenation over the Cu/ZnO catalyst: the contribution of hydrogen spillover

Lin Gao,*[a,b,c] Guoqiang Ding,*[c] Lei Zhu,[c] Zhanqiu Yu,[c] Hongju Li,[c] Guoqiang Li,[d] Yulei Zhu,[a,c] Hongwei Xiang,[a,c] Xiaodong Wen,*[a,c] Yong Yang[a,c] and Yongwang Li[c]

Received 20th December 2023,
Accepted 29th January 2024

DOI: 10.1039/d3dt04268e

rsc.li/dalton

The dimethyl maleate hydrogenation activity of Cu, ZnO-*X* and physically mixed Cu+ZnO-*X* samples was systematically investigated to probe the essential role of ZnO in ester hydrogenation processes. Cu samples exhibited high C=C bond hydrogenation ability with dimethyl succinate as the main product. Comparatively, ZnO was inactive in hydrogenation due to its weak ability to dissociate hydrogen while the C=O group could be activated and adsorbed on the ZnO surface. Interestingly, physical mixing with ZnO significantly improved the C=O hydrogenation activity of Cu samples. The H_2-TPD results reveal the origin of "Cu–ZnO synergy": hydrogen atoms formed on the copper surface can spill over to the ZnO surface and react with the adsorbed C=O group.

1. Introduction

The hydrogenation of esters derived from the corresponding acids holds considerable commercial importance in the production of alcohols due to its broad application in the food, pharmaceutical and textile industries.[1–8] One such essential process is the hydrogenation of dimethyl maleate (DMM), which results in some significant fine chemicals like gamma-butyrolactone (GBL), 1,4-butanediol (BDO), and tetrahydrofuran (THF), as depicted in Scheme 1.[2,7,8] Recently, researchers have dedicated themselves to developing a new environment friendly BDO production process since it serves as the key monomer for manufacturing biodegradable plastics such as poly(butylene succinate) (PBS) and poly(butylene adipate-*co*-terephthalate) (PBAT).[9]

Copper-based catalysts, including Cu/ZnO, Cu/SiO_2, and Cu/Cr_2O_3, have been widely used for ester hydrogenation.[10–12] Many studies suggested that the reaction occurs exclusively on Cu^0 and that the catalytic activity is closely related to the copper surface area (S_{Cu}).[13] However, the specific activity (activity per unit area of Cu) of ester hydrogenation can be altered by using different supports or additives. Studies by Turek *et al.*[10] revealed that the specific activity of the Cu/ZnO catalyst was approximately one order of magnitude greater than that of Cu/SiO_2 and Cu/Cr_2O_3 catalysts during dimethyl succinate (DMS) hydrogenation processes. Likewise, Van de Scheur *et al.*[14] reported that the catalytic performance of the Cu/SiO_2 catalyst was greatly enhanced by adding ZnO in methyl acetate to ethanol hydrogenation. Our own experimental results further confirm that the specific activity of the Cu/ZnO catalyst surpasses those of Cu/SiO_2, Cu/Al_2O_3 and Cu/Cr_2O_3.

The excellent performance of the Cu/ZnO catalyst is generally attributed to the strong metal–support interaction (SMSI) effect, which may lead to the formation of specific active centres such as $Cu^{\delta+}$ ($0 < \delta \leq 1$) or the stabilization of Cu^0 in a morphologically active form.[15–18] Chen *et al.*[19–21] proposed that $Cu^{\delta+}$ might play an essential role in the hydrogenation of DMM by facilitating the adsorption and activation of the carbonyl group. Zhang *et al.*[22] reported that both Cu^0 and Cu^+ phases coexist on the surface of the Cu–Zn–Al catalyst, where Cu^0 and Cu^+ enable the formation of THF and GBL/BDO, respectively. Furthermore, Figueiredo[23] and Mendes *et al.*[24]

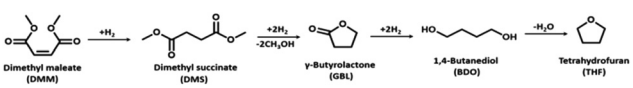

Scheme 1 Reaction pathway for the hydrogenation of dimethyl maleate.

[a]*State Key Laboratory of Coal Conversion, Institute of Coal Chemistry, Chinese Academy of Sciences, Taiyuan 030001, PR China.*
E-mail: gaolin@synfuelschina.com.cn
[b]*University of Chinese Academy of Sciences, Beijing, 100049, PR China*
[c]*Synfuels China Co. Ltd, Beijing, PR China.*
E-mail: dingguoqiang@synfuelschina.com.cn
[d]*Synfuels China Inner Mongolia Technology Research Institute Co., Ltd, Ordos, PR China*

observed that hydrogenation reactions involving dimethyl adipate and oleic acid could take place at ZnO–Cu interface regions where ester groups were adsorbed onto ZnO sites while activated hydrogen atoms were provided by Cu^0 species.

ZnO is generally considered inert in ester hydrogenation, but its polar surfaces have been found to be active in the chemical-sorption of oxygenated compounds such as formic acid and maleic acid anhydride.[25] Studies by Figueiredo *et al.* suggested that ZnO can catalyze the transesterification reaction with alkanol at low temperatures,[23] indicating that ZnO could adsorb and activate ester groups. Lu *et al.* have reported on ZnO's ability to catalyze the hydrogenation of benzoic acid esters into the corresponding benzaldehyde; however, this process requires a high temperature (>400 °C) due to ZnO's weak dissociative adsorption ability towards hydrogen.[26–28] These unique catalytic behaviours indicate that ZnO may play a significant role in ester hydrogenation processes.

In this work, a series of physically mixed Cu+ZnO-*X* catalysts without the metal–support interaction (SMSI) effect were used to investigate the crucial role of ZnO in DMM hydrogenation. The H_2-TPD experimental results presented in this study exhibit that the activated H atoms on copper can spill over onto zinc oxide particles within the physically mixed Cu+ZnO catalyst. This phenomenon leads to the hydrogenation of C=O groups of DMM, resulting in the formation of GBL, BDO and THF. Therefore, unlike previous research studies where a sole copper species (Cu^0 or Cu^+) or an interface between Cu and ZnO particles was considered as the active site for the ester hydrogenation, our study suggests that special active sites such as oxygen vacancies located on ZnO polar surfaces presumably also play a key role in ester hydrogenation processes.

2. Experimental

2.1 Materials

Dimethyl maleate (DMM, analytical grade, 99.5%), gamma-butyrolactone (GBL, chromatographic grade, 99.9%), 1,4-butanediol (BDO, analytical grade, 99.5%), tetrahydrofuran (THF, chromatographic grade, 99.9%), methanol (MeOH, analytical grade, 99.5%), ethanol (EtOH, analytical grade, 99.5%), $Cu(NO_3)_2{\cdot}3H_2O$ (analytical grade, 99%), $Zn(NO_3)_2{\cdot}6H_2O$ (analytical grade, 99%), and Na_2CO_3 (analytical grade, 99%) were purchased from Aladdin.

2.2 Catalyst preparation

The Cu/ZnO catalysts were prepared by the co-precipitation method. A mixed solution of $Cu(NO_3)_2{\cdot}3H_2O$ and $Zn(NO_3)_2{\cdot}6H_2O$ salts was used as the metal precursor and 1 M Na_2CO_3 solution was used as the precipitating agent. Precipitation was performed at 80 °C, and the mixed solution was added to Na_2CO_3 solution dropwise, at pH 7.5. The precipitate was aged for 2 h at room temperature before filtering. The filtered cake was washed with deionized water until no Na^+ was detected in it, and subsequently dried at 110 °C for 12 h. The dried catalysts were calcined at 450 °C for 5 h. The ZnO-1, ZnO-2 and ZnO-3 samples were prepared by the same precipitation method with different calcination temperatures (Table 1). ZnO-4 was prepared by the calcination of zinc acetate ($Zn(CH_3CO_2)_2{\cdot}2H_2O$) at 450 °C.

The physically mixed Cu+ZnO-*X* catalysts were prepared by the mechanical mixing method. The obtained CuO and ZnO samples were pressed and sieved through 200–300 mesh, respectively. The obtained 200–300 mesh CuO and ZnO powders with various weight ratios were added to a beaker with an appropriate amount of butane. Then the obtained mixture was strongly stirred to mix the two solid powders evenly. After the stirring, the butane was evaporated at room temperature. The obtained mixed powder was pressed and crushed through 20–40 mesh for the catalytic performance evaluation.

2.3 Catalytic testing

The DMM hydrogenation and transesterification of all the samples were carried out in the same tubular fixed-bed reactor (i.d. 12 mm, length 600 mm) with 5 g catalyst (20–40 mesh). Prior to the reaction, all the catalysts were reduced *in situ* at ambient pressure with a 10 vol% H_2/N_2 gas mixture at 295 °C for 24 h. The feedstock was introduced into the reactor *via* a syringe pump, mixed with pure hydrogen and then vaporized in a preheater. The reaction products were condensed in an ice-water bath and analysed using an SP-2000 gas-chromatograph (GC) equipped with a flame ionization detector (FID) and a capillary column (DM-WAX, 30 m × 0.32 mm × 0.5 mm). The products were also identified using a GC/MS system (GC6890N/5973MSD, Agilent, USA).

2.4 Catalyst characterization

N_2 isotherms were measured with a Micromeritics ASAP 2020 apparatus at 77 K. Prior to the measurement, the samples were vacuum-degassed at 623 K for 5 h. The total surface area was determined by the BET method. The *t*-plot method was applied to obtain the micropore volume and the external surface area. The pore size distributions were obtained from both the adsorption and desorption branches of the isotherms using the BJH method.

Temperature-programmed reduction (TPR) studies were conducted on a Micromeritics Autochem (2920, USA) with a thermal conductivity detector (TCD). Prior to measurement, the sample (40 mg) was purged under an Ar flow (50 ml min^{-1}) up to 450 °C to ensure an adsorbate-free surface and then cooled to 50 °C. Subsequently, the Ar flow was switched to 10 vol% H_2/Ar mixed gas, and a cold trap with isopropanol–liquid nitrogen slurry was added to condense the water vapor. After the TCD signal returned to the baseline, the reduction was performed at a ramping rate of 10 °C min^{-1} from 50 °C to 400 °C.

Temperature-programmed desorption of hydrogen (H_2-TPD) studies were conducted on a Micromeritics Autochem (2920, USA) with a mass spectrometry (MS) detector. Prior to measurement, the sample (300 mg) was purged under an argon flow (50 ml min^{-1}) up to 450 °C to ensure an adsorbate-free surface and then cooled to 50 °C. The sample was reduced

Table 1 Catalytic performances of catalysts in the hydrogenation of DMM[a]

Samples	KE (Cu LMM)[b] (eV)	S_{Cu} [c] (m^2 g^{-1})	BET of ZnO (m^2 g^{-1})	TOF_{Cu} [d] ($\times10^{-3}$ mol m^{-2} h^{-1})	Conv. (%)	Yield[e] (%)						
						DMS	MeOH[e]	GBL	BDO	THF	BMS	Others[e]
Cu/ZnO	918.9	9.7	—	2.1	100[a]	4.1	27.8	23.8	36.3	5.3	1.5	1.2
Cu	919.5	4.0	—	0.2	100	94.7	0.2	0.8	0.2	0	0	4.1
ZnO-1	—	—	27.1	—	3.1	2.7	0	0	0	0	0	0.4
Cu+ZnO-1[f]	919.5	2.1	27.1	1.9	100	64.6	10.0	14.0	8.6	0.3	2.0	0.5
Cu+ZnO-2[f]	919.5	2.1	19.2	1.7	100	65.6	9.7	14.3	7.0	1.3	1.5	0.6
Cu+ZnO-3[f]	919.5	2.1	6.6	0.8	100	85.4	3.4	8.0	2.0	0.2	0.6	0.6
Cu+ZnO-4[g]	919.5	2.1	12.1	3.6	100	100	27.9	23.0	22.9	20.4	2.2	3.3

[a] Reaction conditions: 210 °C, 4.0 MPa, WHSV = 0.48 or 0.96 h^{-1}, and H_2/DMM = 100 (molar ratio). [b] KE (Cu LMM) = the kinetic energy of Cu LMM measured on a VG MiltiLab 2000 with a Mg Kα radiation. [c] S_{Cu} = specific copper area of catalysts after experimentally measured by the N_2O adsorptive decomposition technique.[32] [d] TOF_{Cu} = turnover frequency which is expressed as the mol of H_2 consumed for the hydrogenation of the carbonyl group of DMS per unit of specific copper surface (S_{Cu}) per hour.[11] [e] MeOH = methanol and others = other products mainly propanol, butanol, *etc.* [f] Calcination temperatures of ZnO-1, ZnO-2, and ZnO-3 samples were 350, 450 and 750 °C respectively. [g] ZnO-4 was obtained from the calcination of $Zn(CH_3CO_2)_2{\cdot}2H_2O$ at 450 °C.

with 10 vol% H_2/Ar mixed gas at 295 °C for 15 min at a heating rate of 1 °C min^{-1}. After this step, the 10 vol% H_2/Ar mixed flow was switched to H_2 for 15 min to saturate H_2 adsorption on the surface of the sample and then cooled to −100 °C under an H_2 atmosphere. Subsequently, the sample was purged with Ar for 30 min to remove weakly adsorbed species, and a cold trap with isopropanol–liquid nitrogen slurry was added to condense the water vapor. After the mass spectrometry (MS) signal returned to the baseline, H_2-TPD was carried out at a ramping rate of 10 °C min^{-1} from −100 °C up to 600 °C.[15,29,30]

The specific copper surface area (S_{Cu}) of the catalyst was obtained according to the improved N_2O decomposition method suggested by Gervasini and Bennici.[11] The experiments were carried out with the same apparatus used for H_2-TPD, and the sample loading was 300 mg. Prior to measurement, *in situ* pre-reduction of the CuO phase to Cu^0 was performed at 295 °C (at a heating rate of 1 °C min^{-1}) under a flowing 10 vol% H_2/Ar mixed gas for 30 min. The reduced sample was then cooled to 40 °C in an Ar flow. The oxidation of surface metal copper to Cu_2O by adsorptive decomposition of N_2O was carried out isothermally at 40 °C in a continuous 0.5 vol% N_2O/N_2 mixed flow for 30 min. After this, the sample was purged in an Ar flow for 30 min, and subsequently, a TPR measurement was carried out as described above. Quantitative H_2-uptakes were evaluated by integration of the experimental TPR curves, based on the previous calibration measurements with CuO (purity >99 wt%) powder. The copper surface area was calculated from these results assuming a copper surface density of 1.47×10^{19} copper atoms per square meter.

Quasi-*in situ* X-ray Photoelectron Spectroscopy (XPS) and X-ray Auger Electron Spectroscopy (XAES) were performed with a Physical Electronics VG MiltiLab 2000 spectrometer equipped with a Mg Kα (1253.6 eV) X-ray source. Prior to each test, the calcined catalyst was reduced under H_2 at 250 °C for 2 h and was transferred to the sample holders in the glove box under N_2 protection. The obtained binding energies were calibrated using the C 1s peak at 284.6 eV as given in ref. 31.

3. Results and discussion

3.1 Cu XPS-Auger spectra of the reduced Cu catalysts

Since metallic and cuprous species possess rather similar binding energies, XAES measurements are necessary to discriminate Cu species.[1] XPS-Auger studies reveal that the kinetic energy (KE) of Cu LMM in the co-precipitated Cu/ZnO catalyst is 0.6 eV lower than that of pure Cu, suggesting the presence of intimate contact between Cu and the ZnO phase.[2] However, the physically mixed Cu+ZnO catalyst exhibits the same KE of Cu LMM as that of pure Cu, indicating that the intimate interaction between Cu and the ZnO phase can be avoided by the physical-mixing method.

3.2 Catalytic performances of catalysts in the hydrogenation of DMM

XPS-Auger studies reveal that the kinetic energy (KE) of Cu LMM in the co-precipitated Cu/ZnO catalyst is 0.6 eV lower than that of pure Cu, indicating an intimate contact between Cu and ZnO phases[31] (Table 1 and Fig. 1), whereas the phys-

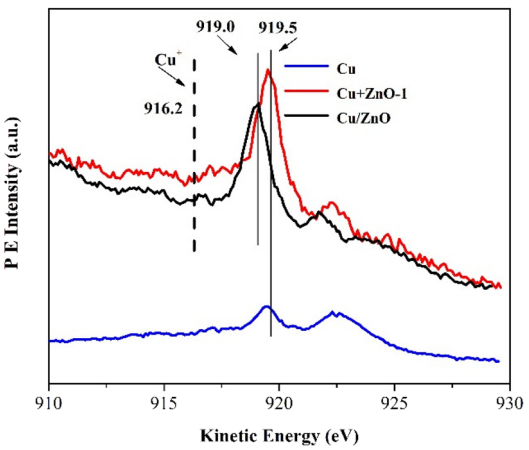

Fig. 1 Cu XPS-Auger spectra of the reduced Cu catalysts.

ically mixed Cu+ZnO catalyst exhibits the same KE of Cu LMM as that of pure Cu, suggesting avoidance of an intimate interaction between both components by this method. Then, the catalytic performance of physically mixed Cu+ZnO-*X* catalysts was evaluated to investigate the essential role played by ZnO in ester hydrogenation. Turek *et al.*[10,11] reported a high reaction rate for the hydrogenation of the C=C bond in DMM to saturated DMS, and the subsequent carbonyl group hydrogenation of DMS to GBL and BDO was determined as the rate-limiting step. The co-precipitated Cu/ZnO catalyst shows high activity in the DMM hydrogenation reaction, and most of the DMM is converted to GBL and BDO (Table 1). A complete conversion of DMM is also obtained over pure Cu. However, the main product is DMS with little formation of GBL and BDO, which suggests the weak hydrogenation ability of pure Cu for the ester group. Pure ZnO is inactive in the hydrogenation reaction, and only about 2% of DMM is converted to saturated DMS without GBL and BDO formation. Interestingly, the activity of Cu for the ester group hydrogenation is significantly improved by physically mixing with ZnO. As shown in Table 1, the yields of GBL, BDO and THF over the physically mixed Cu+ZnO-*X* catalyst are much higher than that of pure Cu. It can be seen that the TOF of the physically mixed Cu+ZnO-1 catalyst is about one magnitude higher than that of pure Cu, which clearly indicates the presence of synergy between the Cu and ZnO particles.

The yield of the ester group hydrogenation product decreases remarkably as the calcination temperature of ZnO increases, as shown in Table 1 (Cu+ZnO-1, Cu+ZnO-2, Cu+ZnO-3). This decrease is likely attributed to the lower BET surface area of ZnO at higher calcination temperatures. Interestingly, the highest yields of methanol (23.0%), GBL (22.9%), BDO (20.4%) and THF (2.2%) were obtained on the physically mixed Cu+ZnO-4 catalyst, though the ZnO-4 sample possessed a relatively lower BET surface area. As shown in Table 1, ZnO-4 is prepared by the calcination of zinc acetate ($Zn(CH_3CO_2)_2{\cdot}2H_2O$) at 450 °C. This suggests that there may be special surface active sites on ZnO-4 formed during the zinc acetate calcination process that contribute to the highest hydrogenation ability. Therefore, it appears that the catalytic performance of the physically mixed Cu+ZnO-*X* catalysts is determined by the surface properties of ZnO.

3.3 Transesterification performances of DMM with ethanol on Cu and ZnO particles

Scheur *et al.*[33,34] reported that the transesterification reaction may occur competitively in the methyl acetate (MA) hydrogenation process, as the desired product ethanol can react with acetate to form acetate and methanol. At low temperatures, the main products are ethyl acetate (EA) and methanol other than ethanol, while a higher temperature is necessary for the formation of the desired product ethanol with a complete conversion of MA. Correspondingly, the transesterification of DES with BDO was also detected in the DMM hydrogenation process with the production of 4-hydroxybutyl methyl succinate (BMS) (Table 1).

Thus, the transesterification of DMM with ethanol was conducted to investigate the active centers for the carbonyl group under the same reaction conditions (210 °C, H_2 pressure 4.0 MPa) applied for DMM hydrogenation (Table 2). Over pure Cu particles, only minimal transesterification products are formed (2.2%) with the main product being DMS, indicating weak adsorption and activation of DMM's carbonyl group on the prepared pure Cu. On the other hand, a high selectivity (82.6%) of the transesterification product is obtained over ZnO, suggesting effective absorption and activation of the carbonyl group of DMM on ZnO's surface. However, since ZnO itself cannot provide sufficient active hydrogen (discussed as follows), desired products such as GBL and BDO could not be obtained.

3.4 Temperature programmed desorption experiment of hydrogen (H_2-TPD)

The H_2-TPD measurement was carried out using a Micromeritics Autochem (2920, USA) with a mass spectrometry (MS) detector to investigate the hydrogen adsorption behavior of various catalysts, and the resultant findings are shown in Fig. 2. A distinct hydrogen desorption peak at *ca.* −40 °C is observed in the H_2-TPD pattern of pure Cu,[29] while only a small peak at *ca.* 340 °C is seen over ZnO. The weak hydrogen adsorption ability of ZnO may be responsible for its

Table 2 Transesterification of DMM with ethanol[a]

Sample	Conv. (%)	Selectivity (%)		
		Product of hydrogenation	Product of transesterification	Others
Cu	100	97.1[b]	2.2[c]	0.7
ZnO-1	26.5	14.3	82.6[d]	3.1

[a] Reaction conditions: 210 °C and H_2 pressure 4.0 MPa. [b] Mainly containing DMS. [c] Mainly containing ethyl methyl succinate (EMS) and methanol. [d] Mainly containing ethyl methyl maleate (EMM) and methanol.

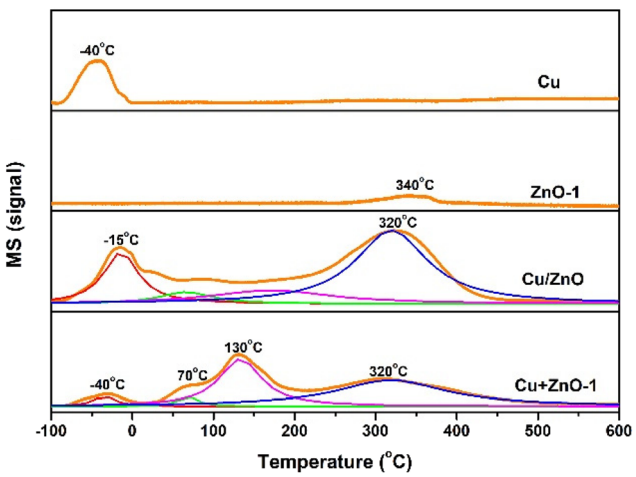

Fig. 2 H_2-TPD profiles of Cu, ZnO-1, Cu/ZnO, and Cu+ZnO-1 catalysts.

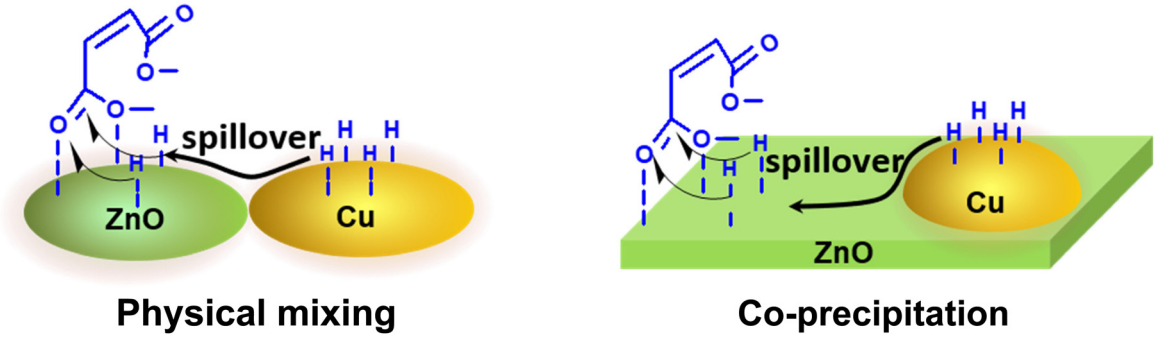

Scheme 2 The possible mechanism of DMM hydrogenation over Cu+ZnO-*X* and Cu/ZnO catalysts.

inadequate hydrogenation capability. Interestingly, the H_2-TPD pattern of the Cu+ZnO-1 catalyst spans a wide range of temperatures; Besides the H_2 desorption peak on the copper surface, there are peaks at about 70, 130 and 320 °C appearing in the H_2-TPD pattern of the Cu + ZnO-1 catalyst which can be attributed to the hydrogen desorption from the ZnO-1 surface.[30] The remarkable improvement of ZnO's hydrogen adsorption ability through physical-mixing with Cu reveals that hydrogen species formed on the Cu surface can spill over onto the ZnO surface; this finding aligns with previous studies.[15] Additionally, the H_2-TPD pattern of the co-precipitated Cu/ZnO catalyst also spans a broad range of temperatures.

3.5 Synergistic mechanism of copper–zinc oxide

For the reason that the intimate contact between Cu and ZnO is avoided, the origin of the synergy in the physically mixed Cu+ZnO-*X* catalyst may not be attributed to the formation or stabilization of specific active centers (Cu^0 and Cu^+) or the specific reaction at the Cu/ZnO interface. Instead, the hydrogen spillover may play a key role in DMM hydrogenation over physically mixed Cu+ZnO-*X* catalysts. As shown in Scheme 2, the activated hydrogen species by metallic copper can migrate to the ZnO surface and then react with the adsorbed ester group of DMM, consequently giving rise to higher yields of desired products such as GBL and BDO.

According to the proposed mechanism, the TOF_{Cu} may be determined by the number of zinc oxide particles surrounding copper particles in the physically mixed Cu+ZnO-*X* catalysts. Therefore, the effects of ZnO contents on TOF were also systematically investigated at 210 °C and 4.0 MPa. A significant increase in TOF_{Cu} was observed at lower ZnO contents (<30%), while TOF_{Cu} is slowly increased with a further increase in the ZnO content (Fig. 3). Upon increasing the ZnO content to 83%, the highest TOF_{Cu}, almost as high as that of co-precipitated Cu/ZnO catalysts (Table 1), is observed (1.97×10^{-3} mol m^{-2} h^{-1}), which is almost as high as the co-precipitated Cu/ZnO catalyst (Table 1). Thus, it is reasonable to speculate that hydrogen spillover may also play a key role in DMM hydrogenation over co-precipitated Cu/ZnO catalysts.

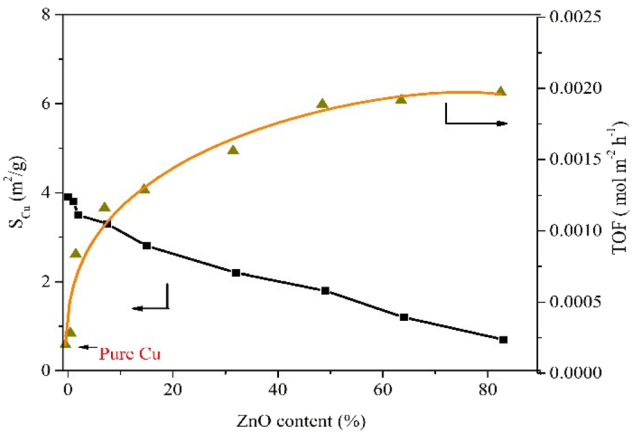

Fig. 3 The effects of ZnO contents on the TOF of copper in the hydrogenation over the physically mixed Cu+ZnO catalyst. Reaction conditions: 210 °C, 4.0 MPa WHSV = 0.48 h^{-1}, and H_2/DMM = 100 (molar ratio).

4. Conclusion

DMM is predominantly converted into saturated DMS with little formation of GBL and BDO over pure Cu. ZnO itself is inactive in hydrogenation reactions due to its weak ability to dissociatively adsorb hydrogen, though the carbonyl group of DMM can be adsorbed and activated by ZnO. In physically mixed Cu+ZnO-*X* catalysts, the activated hydrogen species facilitated by copper can migrate to the surface of ZnO and react with DMM to produce desired products like GBL and BDO. By increasing the ZnO content up to 83%, it was observed that the TOF of Cu reached 1.97×10^{-3} mol m^{-2} h^{-1} which was almost as high as that of the co-precipitated Cu/ZnO catalysts. The H_2-TPD results demonstrated that hydrogen spillover also plays a critical role in the hydrogenation of DMM. This work provides a significant complement for a comprehensive understanding of the catalytic mechanism involved in the ester hydrogenation over Cu/ZnO catalysts; further systematic investigations related to the contribution of hydrogen spillover during the ester hydrogenation process are slated for future research.

Author contributions

Lin Gao: methodology, investigation, formal analysis, validation, data curation, writing – original draft, and writing – review and editing. Guoqiang Ding: investigation, formal analysis, writing – original draft, and writing – review and editing. Lei Zhu: formal analysis and resources. Zhanqiu Yu: formal analysis and writing – review and editing. Hongju Li: formal analysis. Guoqiang Li: formal analysis and resources. Yulei Zhu: project administration, funding acquisition, and supervision. Hongwei Xiang: methodology, conceptualization, funding acquisition, and supervision. Xiaodong Wen: writing – review and editing, project administration, funding acquisition, and supervision. Yong Yang: writing – review and editing, project administration, and supervision. Yongwang Li: writing – review and editing and supervision.

Conflicts of interest

The authors declare that they have no known competing financial interests or personal relationships that could have appeared to influence the work reported in this paper.

Acknowledgements

The authors acknowledge the financial support of the key special project of "Inner Mongolia Revitalization Action with Science and Technology" (No. 2021EEDSCXSFQZD004) and the Clean Combustion and Low-carbon Utilization of Coal Strategic Priority Research Program of the Chinese Academy of Sciences (Grant No. XDA 29000000).

References

1 S. Zheng, K. Zhu, W. Li and Y. Ji, *New J. Chem.*, 2017, **41**(13), 5752–5763.
2 X. Q. Han, Q. F. Zhang, F. Feng, C. S. Lu, L. Ma and X. N. Li, *Chin. Chem. Lett.*, 2015, **26**(9), 1150–1154.
3 J. Pritchard, A. Ciftci, M. W. G. M. (Tiny) Verhoeven, E. J. M. Hensen and E. A. Pidko, *Catal. Today*, 2017, **279**, 10–18.
4 M. A. Sánchez, G. C. Torres, V. A. Mazzieri and C. L. Pieck, *J. Chem. Technol. Biotechnol.*, 2016, **92**(1), 27–42.
5 C. Zhang, Z. Huo, D. Ren, Z. Song, Y. Liu, F. Jin and W. Zhou, *J. Energy Chem.*, 2019, **32**, 189–197.
6 W. Di, J. Cheng, S. Tian, J. Li, J. Chen and Q. Sun, *Appl. Catal., A*, 2016, **510**, 244–259.
7 G. Ding, Y. Zhu, H. Zheng, W. Zhang and Y. Li, *Catal. Commun.*, 2010, **11**(14), 1120–1124.
8 G. Ding, Y. Zhu, H. Zheng, H. Chen and Y. Li, *J. Chem. Technol. Biotechnol.*, 2010, **86**(2), 231–237.
9 P. Jambunathan and K. Zhang, *J. Ind. Microbiol. Biotechnol.*, 2016, **43**(8), 1037–1058.
10 T. Turek, D. L. Trimm, D. S. Black and N. W. Cant, *Appl. Catal., A*, 1994, **116**(1–2), 137–150.
11 J. H. Schlander and T. Turek, *Ind. Eng. Chem. Res.*, 1999, **38**(4), 1264–1270.
12 Y. Shao, K. Sun, Q. Li, Q. Liu, S. Zhang, Q. Liu, G. Hu and X. Hu, *Green Chem.*, 2019, **21**, 4499–4511.
13 M. Mokhtar, C. Ohlinger, J. H. Schlander and T. Turek, *Chem. Eng. Technol.*, 2001, **24**(4), 423–426.
14 F. T. Van de Scheur and L. H. Staal, *Appl. Catal., A*, 1994, **108**(1), 63–83.
15 R. Burch, S. E. Golunski and M. S. Spencer, *J. Chem. Soc., Faraday Trans.*, 1990, **86**(15), 2683–2691.
16 J. Yu, X. Qin, Y. Yang, M. Lv, P. Yin, L. Wang, Z. Ren, B. Song, Q. Li, L. Zheng, S. Hong, X. Xing, D. Ma, M. Wei and X. Duan, *J. Am. Chem. Soc.*, 2024, **146**(1), 1071–1080.
17 Y. Liu, X. Liu, L. Xia, C. Huang, Z. Wu, H. Wang and Y. Sun, *Acta Phys.-Chim. Sin.*, 2022, **38**(3), 2002017.
18 L. Zhang, Y. Wu, N. Tsubaki and Z. Jin, *Acta Phys.-Chim. Sin.*, 2023, **39**(12), 2302051.
19 L. F. Chen, P. J. Guo, M. H. Qiao, S. R. Yan, H. X. Li, W. Shen, H. L. Xua and K. N. Fan, *J. Catal.*, 2008, **257**(1), 172–180.
20 L. F. Chen, P. J. Guo, L. J. Zhu, M. H. Qiao, W. Shen, H. L. Xu and K. N. Fan, *Appl. Catal., A*, 2009, **356**(2), 129–136.
21 E. K. Poels and D. S. Brands, *Appl. Catal., A*, 2000, **191**(1–2), 83–96.
22 Q. Zhang, Z. Wu and L. Xu, *Ind. Eng. Chem. Res.*, 1998, **37**(9), 3525–3532.
23 F. C. A. Figueiredo, E. Jordão and W. A. Carvalho, *Catal. Today*, 2005, **107–108**, 223–229.
24 M. J. Mendes, O. A. A. Santos, E. Jordão and A. M. Silva, *Appl. Catal., A*, 2001, **217**(1–2), 253–262.
25 C. Woll, *Prog. Surf. Sci.*, 2007, **82**(2–3), 55–120.
26 A. Wang, W. Quan, H. Zhang, H. Li and S. Yang, *RSC Adv.*, 2021, **11**(33), 20465–20478.
27 W. Lu, G. Lu, X. Liu, Y. Guo, J. Wang and Y. Guo, *Mater. Chem. Phys.*, 2003, **82**(1), 120–127.
28 W. F. Hölderich and J. Tjoe, *Appl. Catal., A*, 1999, **184**(2), 257–264.
29 J. Tabatabaei, B. H. Sakakini, M. J. Watson and K. C. Waugh, *Catal. Lett.*, 1999, **59**(2/4), 143–149.
30 F. Arena, G. Italiano, K. Barbera, S. Bordiga, G. Bonura, L. Spadaro and F. Frusteri, *Appl. Catal., A*, 2008, **350**(1), 16–23.
31 W. L. Dai, Q. Sun, J. F. Deng, D. Wu and Y. H. Sun, *Appl. Surf. Sci.*, 2001, **177**(3), 172–179.
32 A. Gervasini and S. Bennici, *Appl. Catal., A*, 2005, **281**(1–2), 199–205.
33 P. Claus, M. Lucas, B. Lücke, T. Berndt and P. Birke, *Appl. Catal., A*, 1991, **79**(1), 1–18.
34 F. T. Scheur and L. H. Stall, *Appl. Catal., A*, 1994, **108**(1), 63–83.